FFI-RAPPORT

17/00415

3D printed metamaterial lenses for microwave antennas

–

Stein Kristoffersen
Karina Vieira Hoel

3D printed metamaterial lenses for microwave antennas

Stein Kristoffersen
Karina Vieira Hoel

Norwegian Defence Research Establishment (FFI) 1 March 2017

Keywords

Antenner
Metamaterialer
Linser

FFI-rapport
FFI-RAPPORT 17/00415

Prosjektnummer
504101

ISBN
P: 978-82-464-2902-1
E: 978-82-464-2903-8

Approved by
Tom Thorvaldsen, *Researcher*
Jon E. Skjervold, *Director*

Summary

This report presents the results from a study initialized and financed by «kompetanseområde Materialteknologi» at the Norwegian Defence Research Establishment (FFI). It is an exploratory study on metamaterials, and the work presented here is limited to materials with spatially varying permittivity and their applications to antennas.

Metamaterials are materials with properties that are not readily available in nature. Usually, the special properties arise from structures in the material, which results in electromagnetic waves experiencing unusual or unnatural permittivity and/or permeability when interacting with the metamaterial. These meta properties are usually only present in limited frequency bands.

The authors of this report have previous experience from antenna design using 3D printing. In this work, we use this manufacturing technology to produce blocks of plastic with varying density to demonstrate that we can produce materials with controllable permittivity. This requires a structure with a resolution significantly higher than the wavelength. For our microwave applications with wavelengths down to one centimeter, we require a structure at millimeter scale. Producing such fine structures has recently become possible with the use of modern 3D printers. Simulations and measurements on the plastic blocks show that we can achieve relative permittivity values ranging from close to one (as in air) and up towards the permittivity of 100 percent density of the material being used.

To demonstrate relative permittivity, we designed a number of plastic lenses with spatially varying density and measured the effect on the radiation diagram of an antenna. The example presented here shows a 3dB increase in gain over a relative bandwidth of more than 2:1. In radio systems, the range is proportional to the square root of the transmitted power, and hence a 3dB gain results in more than 40 percent increase in range.

Sammendrag

Denne rapporten oppsummerer arbeidet som er gjort i en utforskende studie om metamaterialer, initiert og finansiert av kompetanseområde Materialteknologi ved Forsvarets forskningsinstitutt (FFI). Temaet her er begrenset til materialer med romlig varierende permittivitet og anvendelser innen antenneteknologi.

Metamaterialer er materialer med egenskaper som ikke er tilgjengelige i naturlige eller naturskapte materialer. Vanligvis fremkommer disse egenskapene ved at materialet har en spesiell struktur som resulterer i at elektromagnetiske bølger utsettes for andre verdier for permittivitet og/eller permeabilitet sammenliknet med naturlige materialer. Metaegenskapene er normalt bare til stede for begrensede frekvensområder.

Forfatterne har tidligere erfaring med antenneutvikling og -produksjon ved hjelp av 3D-printere. I dette arbeidet brukte vi 3D-printing til å produsere blokker av plast med forskjellig tetthet for å demonstrere at vi kan produsere materialer med kontrollerbar permittivitet. Dette krever en struktur som er vesentlig finere enn bølgelengden. For våre mikrobølgeapplikasjoner, med bølgelengde ned mot én centimeter, kreves dermed strukturer ned mot én millimeter. Dette er nylig blitt tilgjengelig ved bruk av moderne 3D-printere. Simuleringer og målinger på plastblokkene viser at vi kan realisere relativ permittivitet som varierer fra ned mot én (som er permittiviteten til luft) opp mot permittiviteten til printematerialet med 100 prosent tetthet.

For å demonstrere varierende relativ permittivitet designet vi et antall linser med romlig varierende tetthet og målte deres påvirkning på en antennes strålingsegenskaper. I eksempelet som presenteres i denne rapporten, blir økt antenneforsterkning på omkring 3dB demonstrert over en relativ båndbredde på mer enn 2:1. For et radiosystem er rekkevidden proporsjonal med kvadratroten av sendereffekten, og 3dB resulterer dermed i over 40 prosent økt rekkevidde.

Content

1 Introduction

This report summarizes a time limited study, which was conducted during the autumn of 2016. The work was financed by a grant of 100.000 NOK given by "Kompetanseområde Materialteknologi".The grant was announced in spring 2016, and this year's topic was metamaterials[1]. Any study topic including metamaterials was valid. Two different proposals where submitted, and our suggested study on "3D printed metamaterial lenses for microwave antennas" was chosen. The announcement text and the application can be found in appendices A and B, respectively.

The main objective and idea for this grant is to build internal competence on technology areas that still are quite new and novel, but considered having a large potential for use in future military applications. The overall goal is to demonstrate new technology and possibilities to the Armed Forces, to improve their systems and operational ability. Moreover, such studies also aim at motivating FFI researchers in their work.

In this report, we will first give a short background and define the objectives of this study, including a brief introduction to metamaterials and 3D printing, as these research areas are central to this work. Thereafter we give a bit more detailed introduction to metamaterials for antennas. Finally, we demonstrate the use of 3D printed metamaterials in antenna applications; two different cases are included. A summary and conclusion of the work is included at the end of the report.

2 Background and objectives

Our background is in electromagnetics and microwave technology. Our daily work is in the research program OPEK, which focuses on topics related to electronic warfare. Due to this, we decided to limit our study to metamaterial topics relevant for microwave applications, and specifically for antennas. We also chose to focus the study on "simple" applications of metamaterials, which should result in better solutions than can be achieved with conventional materials. "Better" in this context could mean e.g. smaller, cheaper, lighter and/or with higher performance.

At the time of the announcement, Karina V. Hoel was in her first year of a PhD program on the topic *"3D printed antennas and microwave components"*. Through this activity we have established experience in designing, simulating, producing and measuring 3D printed antennas. Our suggestion was to take advantage of this capability to study some chosen topics related to

[1] Metamaterials are materials with properties that are note readily available in nature

metamaterials and antennas. Metamaterials were, however, new to us, and we needed to start with studying available literature. A selection of the literature is discussed in Chapter 3. After the literature study we chose two test cases, with the following objectives:

1. To demonstrate that the permittivity of a slab of a material will depend on the density of the material

2. To take advantage of results from item 1, and produce a dielectric lens, which will focus the radiation from an antenna

2.1 Metamaterials

"Meta" is a Greek prefix which can mean "beyond". In general the prefix is used to describe something which is an abstraction of another concept, to expand the original concept. A well-known example is "metadata" which is data describing data. Meta as used in metamaterials, is meant to indicate that the materials have properties which are normally not found in "natural" materials. This can in principle be any property, so one could argue that any artificial composite is a metamaterial.

In this study we will only look at materials which have unusual electromagnetic properties. Our definition of a metamaterial is sort of an average over the following three (which are commonly used in the literature):

- Smith (2000): "Electromagnetic metamaterials are artificially structured materials that are designed to interact with and control electromagnetic waves"

- Pendry (2002): "Metamaterials, materials whose permeability and permittivity derive from their structure"

- Caloz (2006): "Electromagnetic metamaterials are broadly defined as artificial effectively homogenous electromagnetic structures with unusual properties not readily available in nature"

Metamaterials make it possible to realize permeability and/or permittivity according to a pre-defined function of time and/or space. These types of materials can be surfaces or volumes.

Permittivity, normally denoted ε, is a property of a material which describes how the material is affected by, and how it affects, electric fields (E-fields). Correspondingly, the permeability, μ, describes how the material is affected by, and how it affects, magnetic fields (H-fields). Maxwell's equations describe how electromagnetic waves propagate in time and space, and they include ε and μ. Maxwell's equations are shown in appendix C. To go through them in detail is outside the scope of this report, but we will look briefly at some consequences which can be deduced from them [1]; for a more detailed introduction to Maxwell's equations, see [2]. It is possible to develop the equations to get to [1]:

$$\nabla^2\overline{E} = \mu\epsilon\frac{\partial^2\overline{E}}{\partial t^2} \tag{1}$$

$$\nabla^2\overline{H} = \mu\epsilon\frac{\partial^2\overline{H}}{\partial t^2} \tag{2}$$

(1) and (2) leads to two sets of wave equations which describes the electromagnetic (EM) waves in space and time. Further calculations [1] show that the characteristic impedance of a material, η (defined as the amplitude ratio of the E- and H-field), can be described by (3), and the propagation speed, v, of an EM wave through the material can be calculated by (4).

$$\eta = \sqrt{\frac{\mu}{\epsilon}} \tag{3}$$

$$v = \frac{1}{\sqrt{\mu\epsilon}} \tag{4}$$

If we insert μ_0 and ε_0, we get the well-known values for free space:

$$\eta_0 = \sqrt{\frac{\mu_0}{\epsilon_0}} = 120\pi\ \Omega \tag{5}$$

$$v_0 = c = \frac{1}{\sqrt{\mu_0\epsilon_0}} = 3\times10^8\ m/s \tag{6}$$

Different materials have different permittivity. Usually we specify permittivity by $\varepsilon_r = \varepsilon/\varepsilon_0$, where typical values for some materials are shown in Table 2.1 [1].

Material	ε_r	Material	ε_r
Air	1.0006	Polyethylene	2.26
Bakelite	4.8	Polystyrene	2.5
Glass	6.0	Quartz	3.8
Lucite (plastic)	3.2	Dry soil	3.0
Nylon	3.6	Teflon	2.1
Plexiglas	3.45	Water	80

Table 2.1 Permittivity, ε_r, values for some materials [1].

When an EM wave propagates, the direction of propagation will be affected according to Snell's law [1], which states that an EM wave propagating from one material to another will change direction according to (7);

$$n_1 \sin \phi_1 = n_2 \sin \phi_2 \tag{7}$$

Snell's law is illustrated in Figure 2.1.

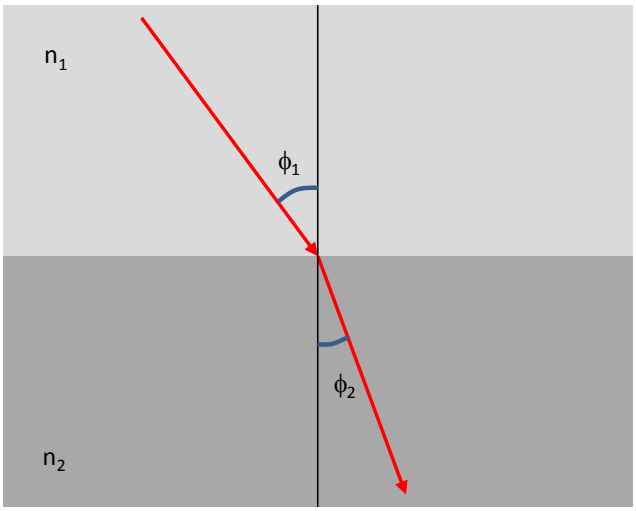

Figure 2.1 Snell's law ($n_2 > n_1$).

The refraction index, n, depends on ε and μ through $n = +\sqrt{\epsilon\mu}$ [1]. So, if we can produce a material in which ε and μ can be made to vary in a controllable manner as a function of the spatial dimensions x, y, z – and maybe even time, we will be able to control how an EM wave is affected by the material.

Other questions, which may arise, include:

- What happens if one of the parameters is negative, resulting in a (seemingly) imaginary refraction index?
- Do all combinations of ε and μ appear in nature?

As it turns out, negative ε or μ is very rare, and no materials with simultaneous negative ε and μ are known.

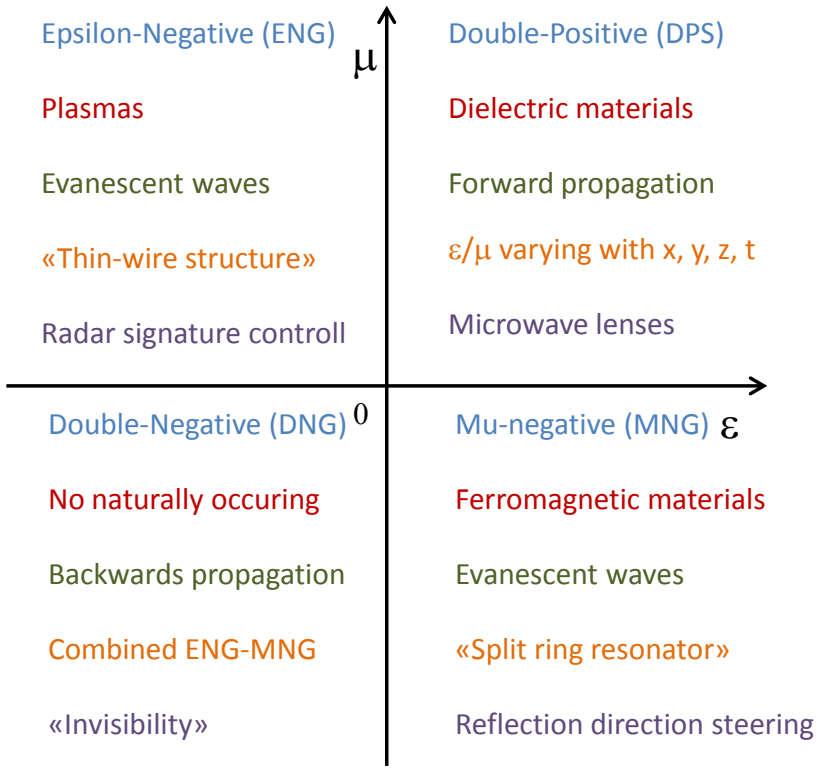

Figure 2.2 The ε–μ space
(blue: sign, red: example material, green: EM wave propagation, orange: example metamaterial type, purple: example application)

The ε-μ space can be established, and can be divided into four sectors/groups, as illustrated in Figure 2.2. This means that all materials can be classified as either double-positive (DPS), epsilon-negative (ENG), mu-negative (MNG) or double-negative (DNG) depending on the sign of their permittivity and permeability.

The work reported here is limited to DPS materials, with spatially varying ε.

2.2 3D-printing

3D printing, or additive manufacturing (AM), is a production technique, where the three-dimensional structure is built layer-by-layer. Hence, instead of starting with a large slab of material, and then removing material to get the wanted geometry and shape, one instead adds the required material. This technique has the potential of producing parts/components with a geometry and functionality that are not possible with more “traditional” production techniques. Moreover, the method also saves a lot of material during production; usually a large percentage of the slab is cut off and wasted during “traditional” production.

The earliest 3D printing technologies can be dated back to the late 1980's. At that time this technology was known as Rapid Prototyping (RP), as the processes were originally conceived as a fast and more cost-effective method for creating prototypes for product development within industry. The first patented application for RP technology was filed by a Dr. Kodama, in Japan, in May 1980 [3]; it was, however, never fulfilled, and the origins of 3D printing can be traced back to 1986, when the first patent by Charles Hull was issued for stereo lithography apparatus (SLA) [4].

In recent years, 3D printing, or 3D rapid prototyping, has expanded rapidly and gone beyond being an industrial prototyping and manufacturing process. One of the main reasons for this is that the technology has become more accessible to small companies and even individuals. More and more systems, materials, applications, services and accessories are emerging every day. One of the great benefits of today's 3D prototyping machines is the ability to produce complicated 3D geometry at roughly the cost of "traditional" plastic parts. As the technology develops, even advanced 3D printed metal parts will soon be available at reasonable prices.

To perform a print, the machine reads the design and lays down successive layers of liquid, powder, or sheet material to build the model from a series of cross sections. These layers, which correspond to the virtual cross sections from the digital model, are joined together or automatically fused to create the final shape. The primary advantage of this technique is its ability to create almost any shape or geometric feature. With the increased popularity of 3D printing technology, many devices with different printing methods have become available.

1) *Stereo Litography* (SLA) is a process that uses a vat of liquid UV curable photopolymer "resin" and a UV laser to build parts one layer at the time. The exposed liquid photopolymers hardens when in contact with air. The build plate then moves down in small increments and the liquid polymer is again exposed to light. The process repeats until the model has been built [7].

2) *Mask Image Projection Based Stereo lithography* is a technique where a 3D digital model is sliced by a set of horizontal planes. Each slice is converted into a two-dimensional mask image. The mask image is then projected onto a photo-curable liquid resin surface. Light is projected on the resin to cure it in the shape of the layer.

3) *Fused Deposition Modeling* (FDM), also known as extrusion deposition, is the most common 3D printing technology. In this technique, thermoplastics are allowed to be melted, layered and reset to create strong and functional parts. Resolution and surface finish are trade-offs as compared to stereo lithography (SLA) [6].

   Various polymers can be used in FDM technology. New thermoplastic materials are constantly being identified and produced in filament form for FDM: ABS (Acrylonitrile Butadiene Styrene), PC (Polycarbonate) PLA (Polylactic Acid), HDPE (High Density

Polyethylene), PC/ABS, PPSU/PPSF (Polyphenylsulfone), Aliphatic polyamides (nylon), PEI/ULTEM (Polyetherimide), PVA (Poluvinyl acetate), PS (High Impact Polystyrene), LDPE (Low Density Polyethylene), PET (Polyethylene Terephthalate), PET mixed with chalk or wood fibers (Laybrick laywood), PHA (Polyhydroxyalkanoates). ABSplus is a production-grade thermoplastic that gives models the ability to perform just like production parts in real-world functional testing.

FDM begins with a 3D computer model in the STL (STereoLithography) file format, which is a collection of many small triangles defining the 3D plot of the solid's surface. Significant amounts of time and material can be saved by reducing the infill percentage which also controls the dielectric constant and loss tangent. The printer constructs the object by extruding plastic while following the code paths calculated from the STL file [6].

The material is extruded through a small hole in the print nozzle. By adjusting the material feed rate and print speed, the thickness can be controlled while also eliminating space between lines which prevents crevices from causing problems when liquid conductive paste is applied. After each layer, the nozzle is moved up by a fixed amount.

4) *Polyjet technology* is similar to ink jet printing, but Polyjet prints jet layers of curable liquid photopolymer onto a tray creating three-dimensional objects. The layers are approximately 0.025 mm thick. The heads are instantly followed by a curing UV light so that, layer by layer, a fully polymerized object is built [8].

5) *Granular Materials Binding* is a technique that fuses parts of the layer, and then moves the working area downwards, adding another layer of granules and repeating the process until the piece has built up. This process uses the unfused media to support overhangs and thin walls in the part being produced. A laser is typically used to sinter the media into a solid. Among the granular materials binding techniques the most common are *Selective Laser Sintering (SLS), Selective Laser Melting (SLM), and Electro Beam Melting (EBM)* [9].

   SLS is an additive manufacturing technique that uses a high power laser (for example carbon dioxide laser) to fuse small particles of plastic, metal (direct metal laser sintering), ceramic or glass powders, and binding them together to create solid structures.

   SLM uses 3D CAD data as a digital information sources and energy in the form of a high-powered laser to create three-dimensional metal parts by fusing fine metallic powders together.

EBM manufactures parts by melting metal powder layer by layer with an electron beam in a high vacuum.

6) *Laminated Object manufacturing* is a process where a sheet is glued to a substrate with a heated roller and cut to the desired dimensions with laser. Laser cross hatches the non-part area to facilitate waste removal. The platform with the completed layer moves down, and a fresh sheet of material is rolled into position. The platform moves up into position to receive the next layer. The process is repeated until the object is finished [10].

Figure 2.3 shows a summary of the different 3D printing processes available, as presented above. The highlighted sections are the different technologies we have tried. We have used several different FDM printers (black), such as Fortus 400mc, Ultimaker 2, and Makerbot. PolyJet (yellow dotted) and SLA (yellow) parts were printed using the Connex 500 and Form 1 respectively. SLS (blue) parts were printed using EOS Formiga P 110. In this project, the 3D printing material technologies that is used is SLS, using the PA2200 material from EOS.

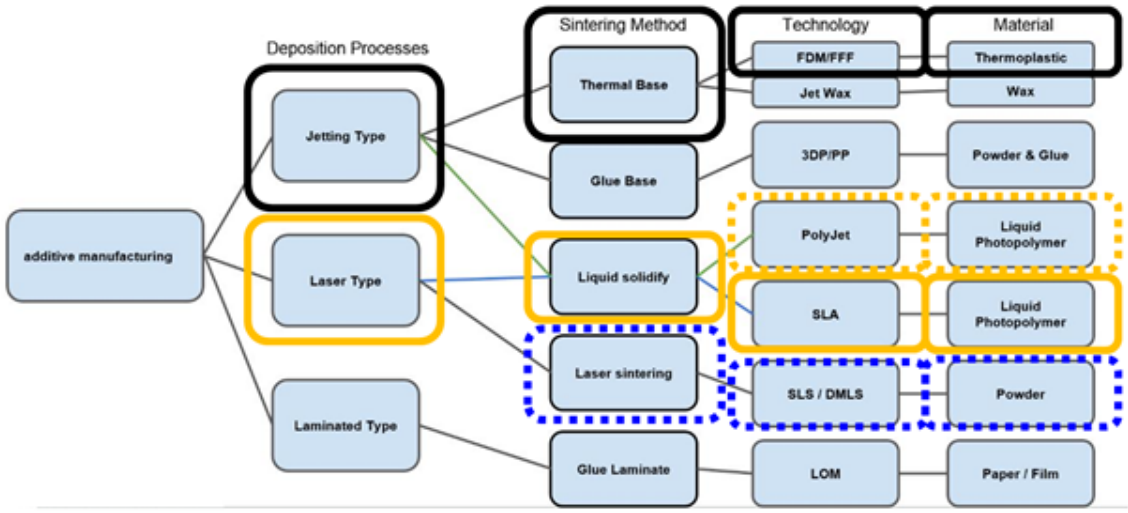

Figure 2.3 Summary of different 3D printing processes [5].

In general, 3D printing provides the possibility to engineer small discrete shapes (unit cell) into the material structure, which has given rise to the idea of tailoring the material properties to suit specific needs. As long as these unit cells are sufficiently small compared to the wavelength of an electromagnetic signal, they appear to the signal as a continuous surface or volume. This allows engineers to manipulate wave propagation by arranging the unit cells in different ways and tune each cell on command. It has been demonstrated that one can achieve negative permeability by stacking periodically ring-resonators, and thin wire structures into the material. Thus, a potential for creating different metamaterials with a combination of plastics and metals is very large. A technology known as molded interconnect devices (MID) is an injection-molded

thermoplastic part with integrated electronic circuitry that provides this capability. This technology merges plastic substrate with circuit traces into a single part by using different processes, such as laser direct structuring (LDS) and 2-shot molding technologies [11].

3 Literature study – metamaterials and antennas

The literature on antenna applications of metamaterials is increasing rapidly, and recently many microwave and antenna conferences have included tracks specifically dedicated to this topic. In this section we present some of the available literature, with emphasis on applications relevant to microwave lens design.

3.1 Gradient index dielectrics

Gradient index dielectrics are materials with spatially varying permittivity. This is essentially the meta-property which allows for totally new design possibilities. Gradient index dielectrics have been manufactured in number of ways, e.g. by producing rings of different plastics which fit into each other, by drilling holes of varying size or density in a slab of compact plastic material, or combinations of dielectrics and metal grids. All of these “traditional” design methods have been cumbersome, and in practice resulted in high loss and/or rough discrete permittivity gradient. Recently additive manufacturing, or 3D printing, has become mature, and many different processes, which employ various dielectric materials, are now available. Many recent publications have studied the electromagnetic properties of variable density 3D printed plastic objects of different designs. Isakov et al. [12] looked at EM properties of different patterns of ABS plastic of different color (and permittivity). Garcia et al. [13] demonstrated controllable permittivity using air gaps in the plastic, and studied the effect of orientation of air channels. The study by Castles et al. [14] is a comprehensive study on how structures in the different composites affect the EM properties. Figure 3.1 shows 3D printed objects from these three studies, used for measuring EM properties.

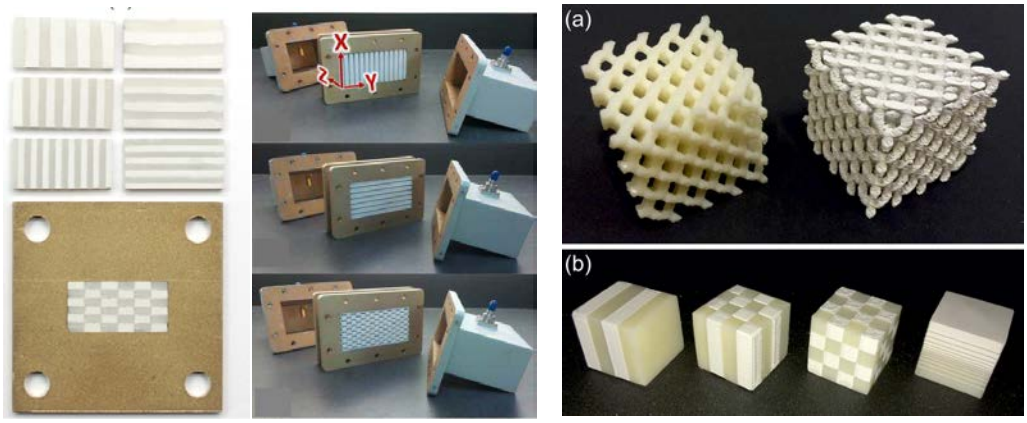

Figure 3.1 3D printed objects prepared for measuring EM properties (from [12], [13] and [14] respectively)

Both studies demonstrate that 3D printers can produce materials with relative permittivity ranging from about 1.2 up to the relative permittivity of the plastic being used for printing. The resolution and orientation of the composite pattern is also shown to be an important factor.

3.2 Microwave lens designs

Microwave lenses have been studied and designed for more than fifty years. A comprehensive coverage of the topic is outside the scope of this report. We will look at two specific published examples:

1. A so-called Luneberg lens [15]; we used a similar method to produce variable density plastic, see Section 4

2. A flat lens [16] using transformation optics for design; similar to the lens we design in Section 5

Both of these lenses were fabricated with 3D printers. Our design could be said to be a mix, or a combination, of the two.

A Luneberg lens is a spherical structure with refractive index (n), or the relative permittivity (ε_r) depending on r, i.e. the distance from the center of the sphere, according to [15],

$$n(r)^2 = \varepsilon_r(r) = 2 - \left(\frac{r}{R}\right)^2 \qquad (8)$$

In (8), n is the refraction index, ε_r is the permittivity, R is the total radius of the lens and r is the distance from the lens center.

Liang et al. [15] achieve the varying ε_r by varying the density of the plastic being used to print the lens. The variable density is achieved using a fine grid, with variable size plastic cubes at the

grid intersections. This is illustrated on the left side of Figure 3.2. The plot on the right side of the figure shows how ε_r depends on the cube size.

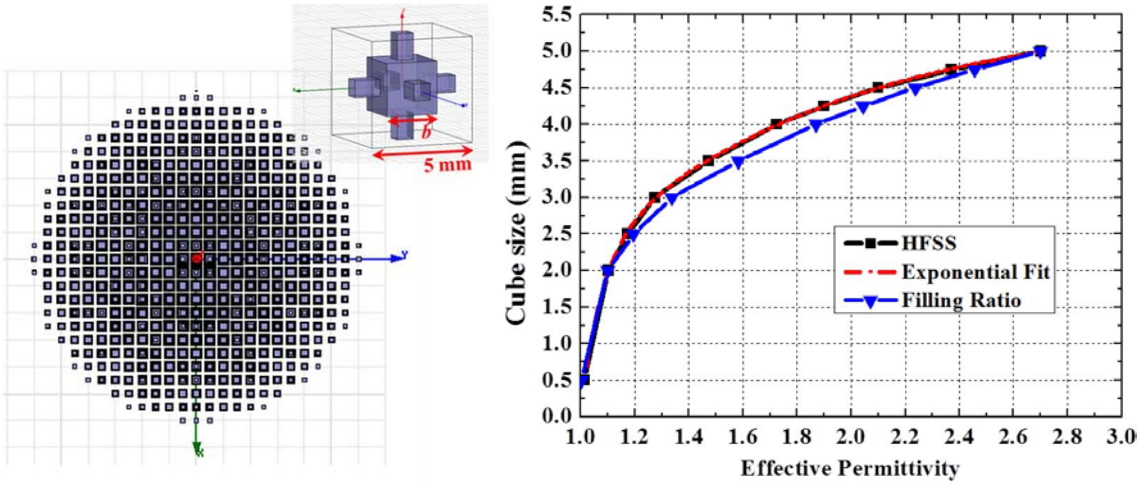

Figure 3.2 3D printed structure to produce variable ε_r [15].

Figure 3.3 shows the 3D printed Luneberg lens. It was manufactured using an Objet Eden 350 polymer jetting printer. For convenient removal of support material, each layer of the lens was produced separately, and the whole structure was assembled by mounting 22 layers together. The left side of the figure is a cross section of the lens, to reveal the spherically varying density of the plastic material. The right side shows the full lens mounted together with a waveguide feed antenna for measurements. The structure is cubic for simpler manufacturing and mounting, but the plastic density outside the sphere is low enough to appear as air to the electromagnetic wave. Antenna gain and beam width were measured to be within 1dB of simulations over the 8-12 GHz frequency band.

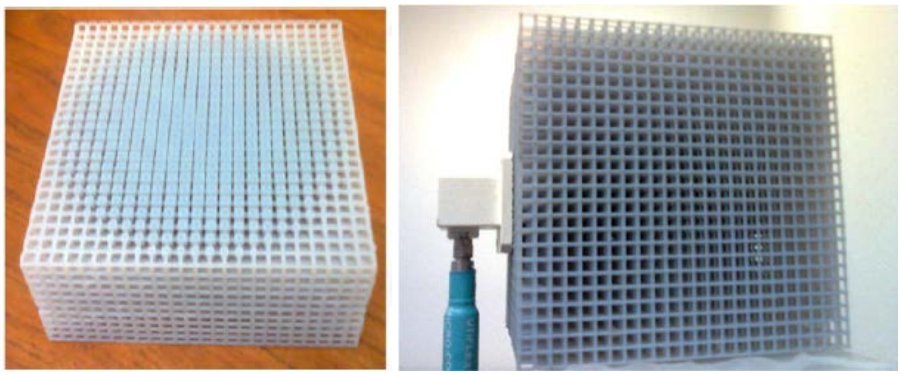

Figure 3.3 3D printed Luneberg lens, cross section to show the variable density structure (left), measurement setup with waveguide feed antenna (right) [15].

Zhang et al. [16] presented a flat (18.5mm) gradient index (GRIN) lens, which is fabricated using a 3D printer employing FDM. A Makerbot Replicator 2X printing with thermoplastic polylactic acid was used. The lens consists of six concentric rings, each with different homogenous ε_r, ranging from 1.3 to 2.6, as seen on the left side of Figure 3.4. For this type of lens the refractive index or permittivity versus radial distance is expressed as [17],

$$n(r)^2 = \varepsilon_r(r) = \left(n_0 - \frac{\sqrt{L^2 + r^2} - L}{t}\right)^2 \tag{9}$$

In (9), n is refractive index, ε_r is relative permittivity, n_0 is refractive index for 100% density, r is the distance from the lens center, L is the focal distance, and t is the lens thickness.

The lens itself can be seen on the right side of Figure 3.4. In this case the varying density of the plastic material is 2D, with gradient in the radial direction only. In the z-direction there is no grid structure. This results in a 2D metamaterial, but it eases production considerably. Since there are no overhanging structures, there is no need for support material, which needs to be removed after manufacturing. The lens shown in Figure 3.4 was measured to have gain between 8 and 10 dB over the frequency range 12 to 18 GHz

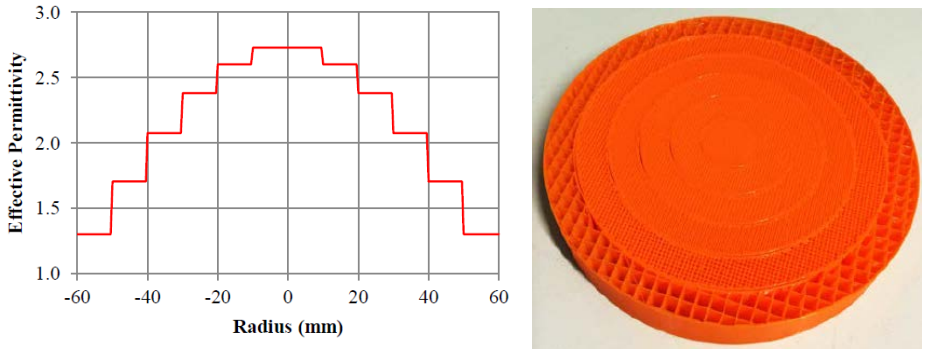

Figure 3.4 3D printed flat lens with discrete step gradient index

In our work, we opted to use the grid structure from [15] to produce a flat lens similar to the one presented in [16], but with continuously varying ε_r.

3.3 Other antenna related metamaterials and applications

Our work was focused on microwave lens design using gradient index materials utilizing 3D printed objects with variable density dielectric materials, as described in sections 3.1 and 3.2. There is however a number of other ways in which metamaterials have been applied to antenna design. Many of them will be briefly described here.

A very interesting application for metamaterials is radar signature control. According to Varga [18], if you construct a surface consisting of controllable circuit components (somehow), then the strength and direction of a reflected EM wave can be controlled through controlling the

circuit elements. Chambers and Tennant [19] demonstrate how this concept can be utilized to design a narrow band programmable (i.e. on/off) absorber of EM energy. They call this a phase-switched screen (PSS). The same authors suggest that wind farms that interfere with radar should use PSS surfaces tuned to the frequencies of the air traffic control radar in [20].

Normally, when an antenna is designed for a given application, one starts with a number of requirements for e.g. beam width, gain, power handling, frequency range etc. For many types of conventional antennas this results in a rather strict requirement for antenna size. For many applications, however, small size or weight is paramount, and antenna miniaturization has been an important research subject for decades. Metamaterials have potential for use in antenna miniaturization, and Dong and Itoh [21] give a comprehensive overview of this topic.

Many antennas require a protective "box" around them for physical protection against weather, debris, etc. This protective box is normally referred to as a radome. The radome needs to be durable, and often the shape is determined by the platform it is mounted on (e.g. on an air plane). Ideally the radome should not affect the performance of the antenna inside in a negative way, and normally one aims for a radome which is as transparent as possible for the frequency range of the antenna. Chamanara and Caloz [22] present a concept for a perfectly matched layer (PML), which does not refract EM waves, regardless of the incidence angle. In [23] a similar idea is applied to the radome of a radar guided missile to minimize the effect of the radome on tracking accuracy. Michishita and Yamanda [24] take the metamaterial based radome design one step further, and present a concept for mobile base stations, which can utilize much simpler antennas than base stations with regular radomes.

These metamaterials can all be said to somehow be space- and time-variable surfaces. This is also the only type of metamaterial which has found commercial applications (as far as we know), as will be described in more detail in Section 3.4.

In addition, a number of more specific, detailed applications of metamaterials in antenna design have been presented. These include mitigating known limitations in current designs, including signal processing in the antenna hardware, shaping the antenna in new ways, making antennas with controllable features, and so forth.

3.4 Commercial application

There is a limited number of reported commercial applications of metamaterials. The most notable is probably the antennas developed by the company Kymeta [25]. Kymeta offers planar satellite communication antennas, which can track the satellite electronically. The product, called mTenna, is shown in on the left side of Figure 3.5. Kymeta is a spin-off company from Intellectualventures, which invented the MSA-T (Metamaterial Surface Antenna Technology). Beam steering is accomplished through altering the surface properties of the antenna electronically. The principle of operation is illustrated in Figure 3.5 [26].

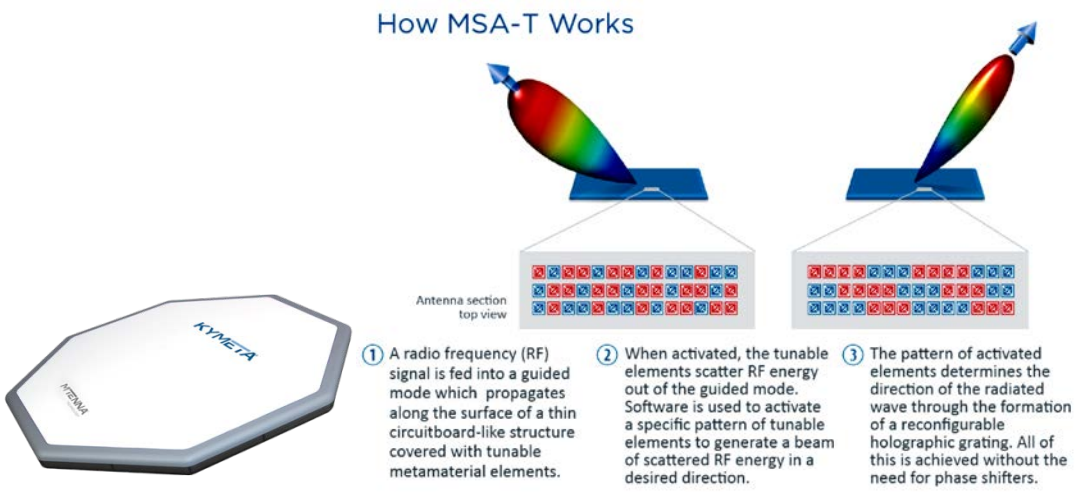

Figure 3.5 Kymeta mTenna (left) and working principle of MSA-T (right)[25] [26].

The flat antenna panels allows for much easier antenna integration on carrier platforms. An example is shown in Figure 3.6, which shows a typical conventional yacht superstructure on the left, and a potential design based on flat panel antennas on the right.

Figure 3.6 Yacht superstructure with conventional antennas (left) and with Kymeta flat antenna panels (right) [26]

Echodyne is another company which offers a metamaterial based planar antenna with electronic beam steering [27]. Their MESA (Metamaterial Electronically Scanning Array) is offered as an alternative to mechanical scanning or phased arrays in radar applications. Echodyne has several radar products operating in different frequency bands. Their designs are small and low weight, and applications on aircraft, cars, on ground and in particular on UAVs are advocated by the company. MESA and mTenna seem to rely on similar principles of surface currents being affected by a metasurface with controllable characteristics.

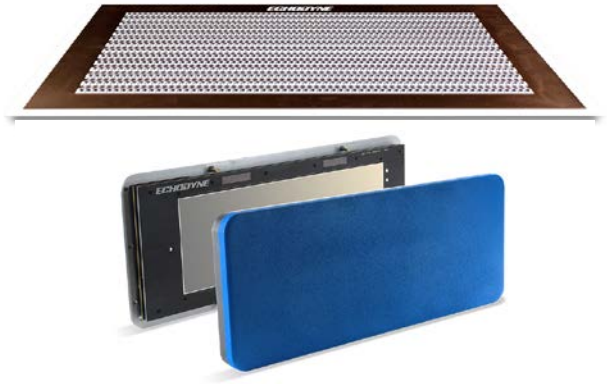

Figure 3.7 Metasurface for Echodyne MESA antenna (top) and K band radar for airborne detect and avoid based on MESA (bottom) [27].

4 Test case 1: Spatially variable permittivity through varying the density of a dielectric material

In this first test case we investigate the spatially variable permittivity by varying the density of a dielectric material. From Table 2.1, we find that air has $\varepsilon_r \approx 1$, and the other materials have $\varepsilon_r > 1$. The hypothesis tested in this test case is the following:

> "*If you produce an object from a material with a certain ε_r, the effective ε_r of the object, as seen by an electromagnetic wave, depends on the density of the material used to produce the object. Also, the dependency is systematic and predictable. This holds even if the density variation is discrete, as long as the resolution is significantly higher than the wavelength of the EM wave*"

If the above is true, it becomes possible to program the ε_r to any value between 1 and the ε_r of the material as a function of the three spatial dimensions, x, y and z. The hypothesis has been proven for certain cases, as reported in Section 3 above. In our case, we want to prove this hypothesis for the same type of structure as was used in [15], but for a different plastic and 3D printing process. Also, in [15] the grid was printed layer-by-layer and mounted afterwards. We wanted to produce the whole object in one print.

To test this we designed a fine grid structure (inspired by [15]) with variable size cubes at each grid intersection. The concept is illustrated in Figure 4.1, where the figure to the left shows one cube unit with intersections to the adjacent cubes, and the figure to the right displays the

resulting lattice grid from intersecting the cube units in the three spatial directions. The plastic of choice for this study was a nylon type called PA2200 (from EOS).

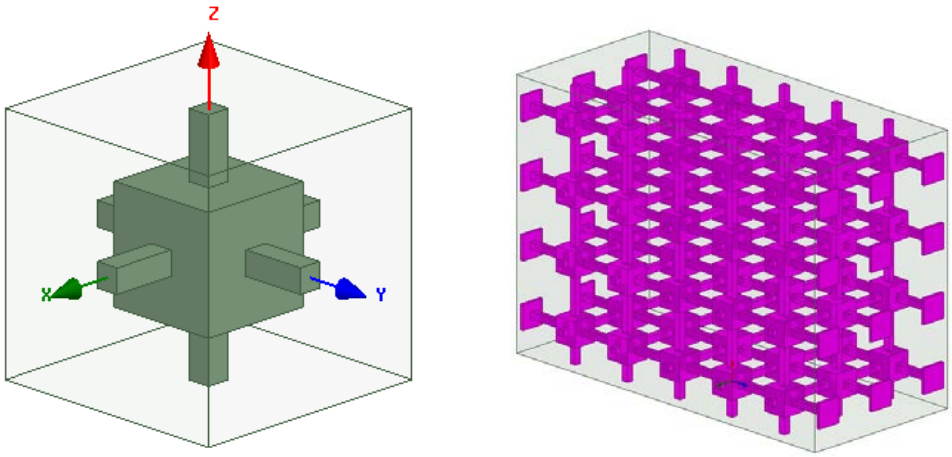

Figure 4.1 Metamaterial with varying permittivity, with a lattice grid structure built up by unit cubes intersected in all three spatial directions. The permittivity of the material is altered by varying the unit cube size.

4.1 Simulations

To test if the lattice structure does, in fact, provide the expected dependence of ε_r on material density, we simulated the ε_r of different lattices with different cubes sizes, as shown in Figure 4.2.

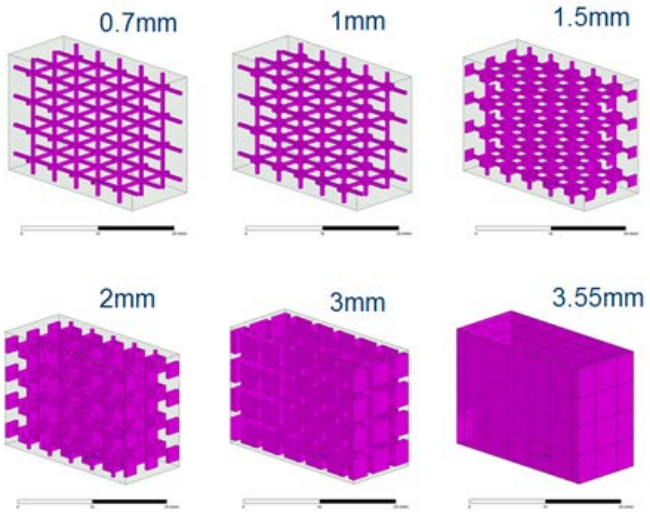

Figure 4.2 3.55x3.55x3.55mm grid of 0.7mm line thickness with cubes at each intersection. The cube size varies from 0.4mm to 3.55 mm.

The ε_r value for a given material is often not readily available and typically not regarded as a primary parameter. Also it depends strongly on any pollutants or additives, and on the achieved density of the material (which is of course the property we seek to exploit in this work). We were first given to believe that the PA2200 material we used has $\varepsilon_r \approx 3.6$. When we measured on a maximum density sample, we found $\varepsilon_r \approx 2.5$. This led us to do an extended literature search. As it turns out, previous work and 3D printer manufacturers provide different values for ε_r for PA2200. The stated ε_r values range from 2.73 in [28] to 2.9 in [29]. The original value of $\varepsilon_r \approx 3.6$ seems to be for a different version of PA2200 which is mixed with glass. Due to this we used $\varepsilon_r = 2.8$ for 100% density plastic in our simulations.

For all simulations we used the High Frequency Electromagnetic Field Simulation Software (HFSS) from Ansys. We designed the 3.55 mm grid of 0.7 mm thickness plastic wire with various cube sizes on the intersections (as shown in Figure 4.2). The ε_r of the plastic was set to 2.8, and the resulting apparent ε_r for the whole grid structure was simulated for the different cube sizes. Resulting ε_r versus frequency is shown in Figure 4.3, clearly demonstrating that the effective ε_r as seen by the EM wave is indeed closely connected to the density of the plastic material. The lowest curve is close to 1, i.e. the ε_r for air, and the top curve is close to $\varepsilon_r = 2.8$ as it would be for compact slab of the nylon material. Any ε_r in between is available through choosing the correct cube size.

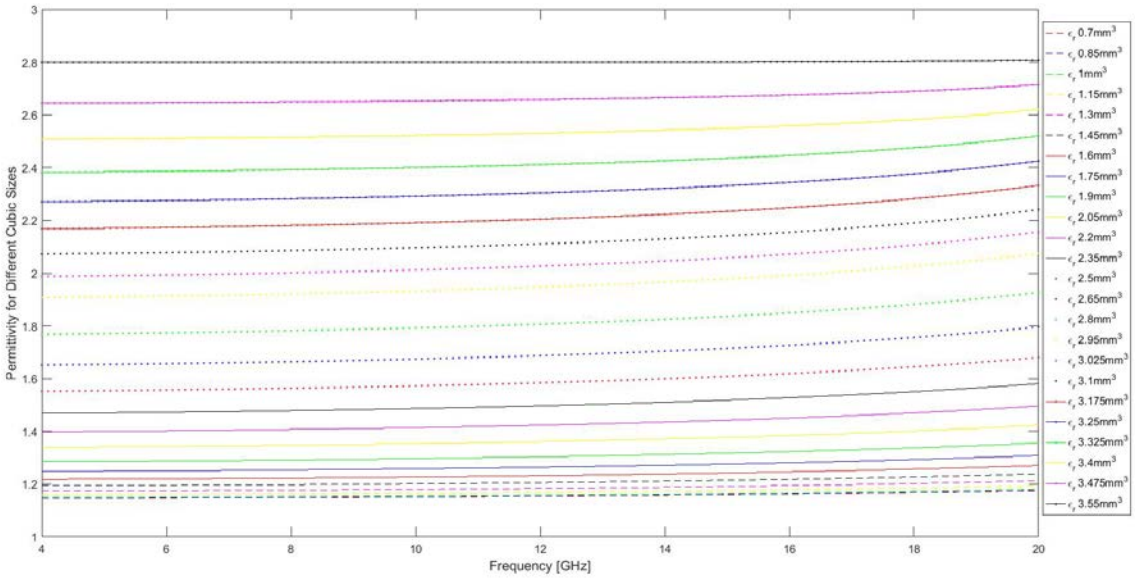

Figure 4.3 Simulated ε_r for different cube sizes using $\varepsilon_{r,max} = 2.8$.

As stated above, there is an inherent uncertainty in what the maximum achievable ε_r is when not every detail of the material is known beforehand. When accurate simulations are needed for e.g. pre-production optimization, a better approach could be to first measure the maximum achievable ε_r on a 100% density material sample, and to use this value in subsequent simulations. The resulting simulated ε_r when following this procedure is shown in Figure 4.4.

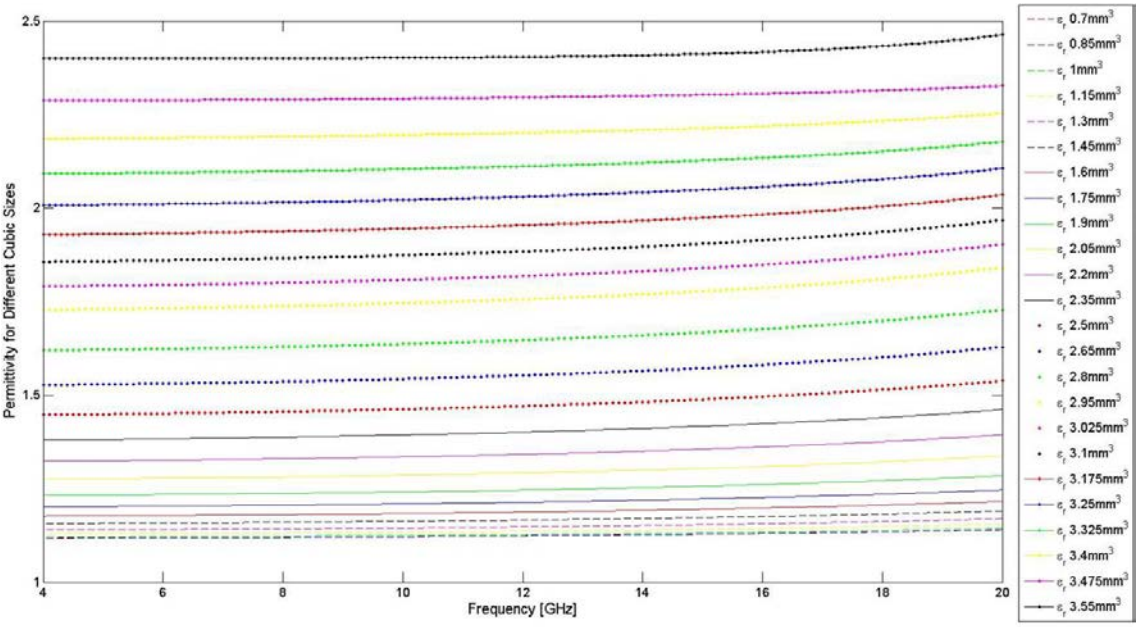

Figure 4.4 Simulated ε_r for different cube sizes using $\varepsilon_{r,max} = 2.4$.

4.2 Measurements

To verify the simulations we produced a number of blocks with different cube sizes. The permittivity ε_r of the produced materials were measured using the N1500A materials measurement software and the PNA N5245A network analyzer from Keysight Technologies, and an X-band waveguide (8.2-12.4GHz). The measurement set-up is shown in Figure 4.5. The different density blocks are inserted into a metal frame as shown in the zoom in the figure. When the two blocks of the analyzer set-up are connected (with the metal frame containing the object in between), the network analyzer can measure the ε_r of the object.

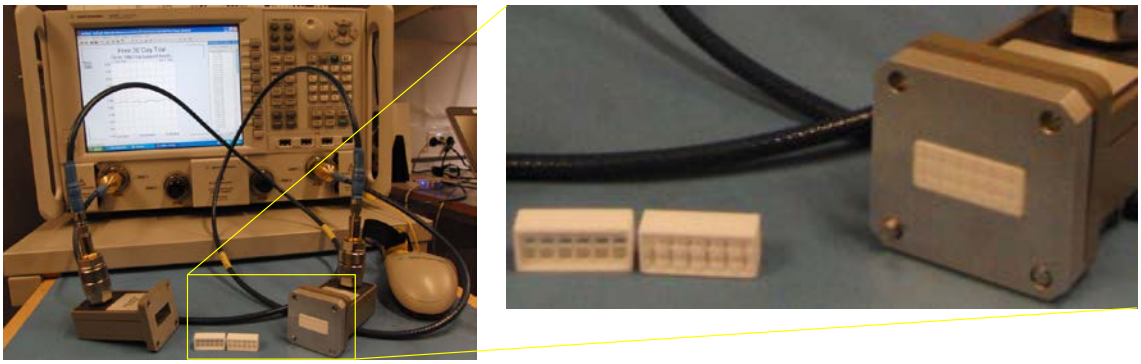

Figure 4.5 Measurement set-up for ε_r measurements.

To produce the actual blocks shown in Figure 4.2, it was necessary to add a robust frame around the lattice, as displayed in the left part of Figure 4.6. The influence on the permittivity of three different versions of the frame is shown on the right side of Figure 4.6; 1) wall thickness of 1 mm (red curve), 2) wall thickness of 0.7 mm (blue curve), and 3) checkerboard wall of 0.7 mm (green curve). As can be seen, the different types of frame have only a small effect on the minimum ε_r, with a difference in permittivity of only around 0.05. The best frame is the checkerboard wall of 0.7 mm (green curve) as also shown on the left side of Figure 4.6. However, due to limitations of the 3D printer and the production of the material objects, the frame with a 1 mm wall thickness (red curve) was chosen.

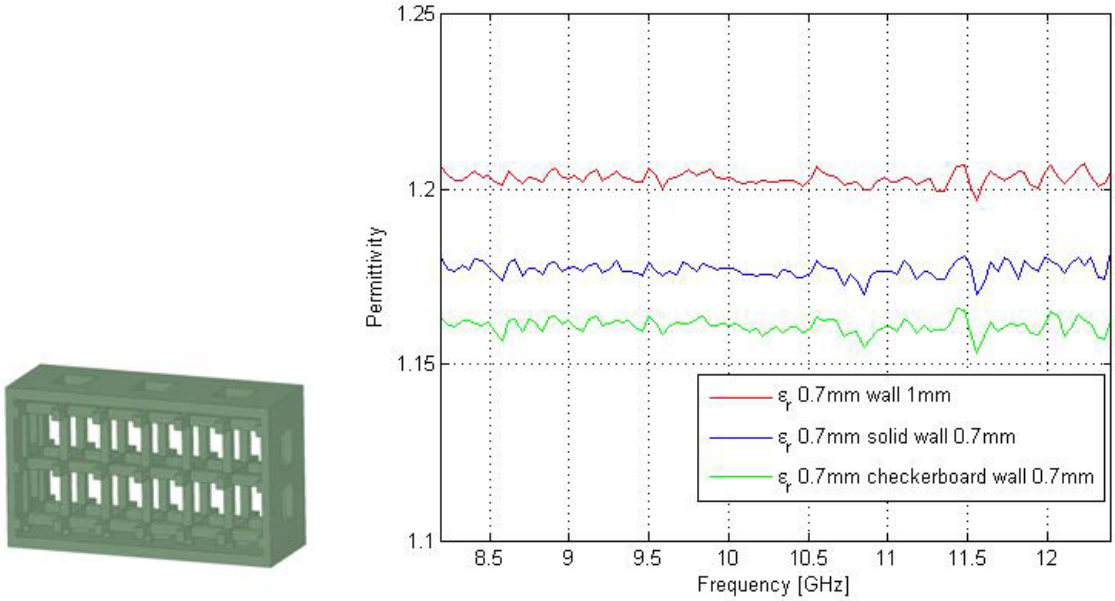

Figure 4.6 Minimum density test object, HFSS drawing 0.7mm checkerboard wall (left) and simulated ε_r for three different frame configurations.

A total of 24 test blocks with different size squares at each grid crossing were measured. The results are shown in Figure 4.7. Comparing the measured permittivity values with the simulated values in Figure 4.3, we observe two main discrepancies:

1. The minimum measured ε_r values are *higher* than the simulation values. The main reason for this is probably the 1 mm frame around the block.

2. The maximum measured ε_r values are *lower* than the original simulation values. The main reason for this is probably related to the printing process not achieving 100% density. If we compare to Figure 4.4 this becomes less of an issue.

The end result is that the span in measured ε_r that we achieved is somewhat lower than simulations led us to expect; values in the range from 1.25 to 2.45 rather than from 1.15 to 2.8. Even so, the main result from the measurements is that the correspondence between cube size, and hence material density, is indeed as expected: Higher density results in higher ε_r, and variable density can be used to produce a lens effect.

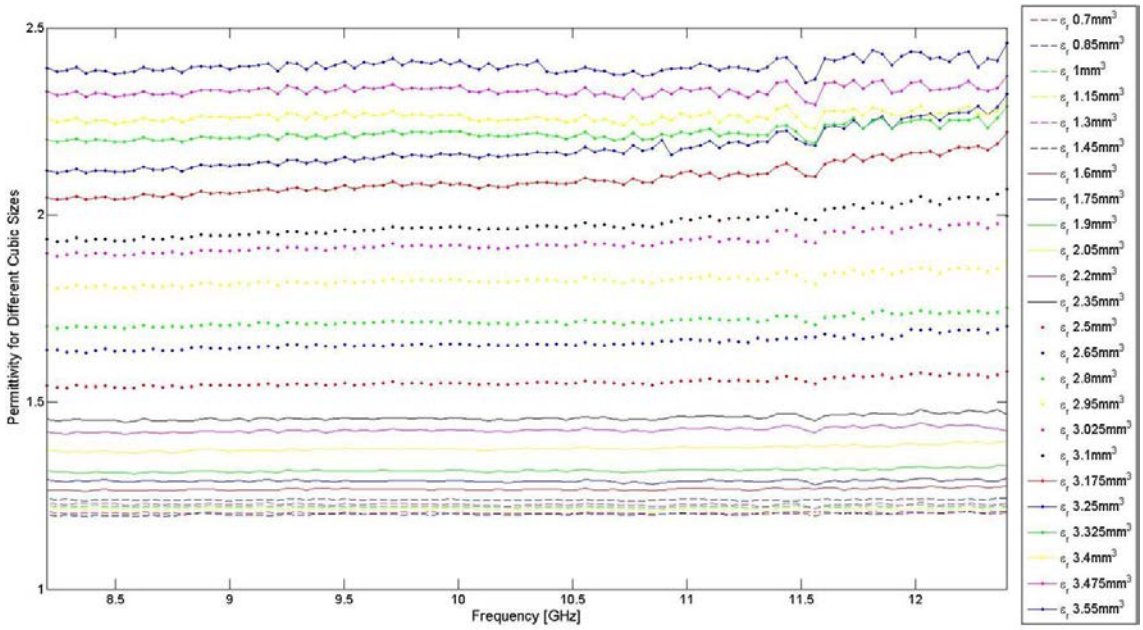

Figure 4.7 Measured ε_r for different density test blocks.

5 Test case 2: Implementation of a 3D printed dielectric lens

Test case 1 verified the basic relationship between material density (or cube size) and ε_r, and pointed out some important differences between theory, simulations and reality. The aim of test case 2 is then to demonstrate a practical application of spatially programmable ε_r – a lens to focus the radiation from an antenna to produce a narrower antenna beam, and hopefully to increase the main beam gain.

The idea is illustrated in Figure 5.1, where the radiation from an antenna can be illustrated conceptually as radially oriented beams originating from the antenna phase center (top of Figure 5.1). In theory, a dielectric lens, which aligns all the beams based on the curvature of the intersecting surfaces, can be designed (middle of Figure 5.1). In reality, such a lens will have to be very thick, and hence also very lossy. The theory of transformation optics tells us that the function of any traditional curved lens made of homogenous material can be replicated by a flat lens with spatially varying ε_r. This was discussed in Section 3.1, and it is illustrated by the bottom drawing in Figure 5.1.

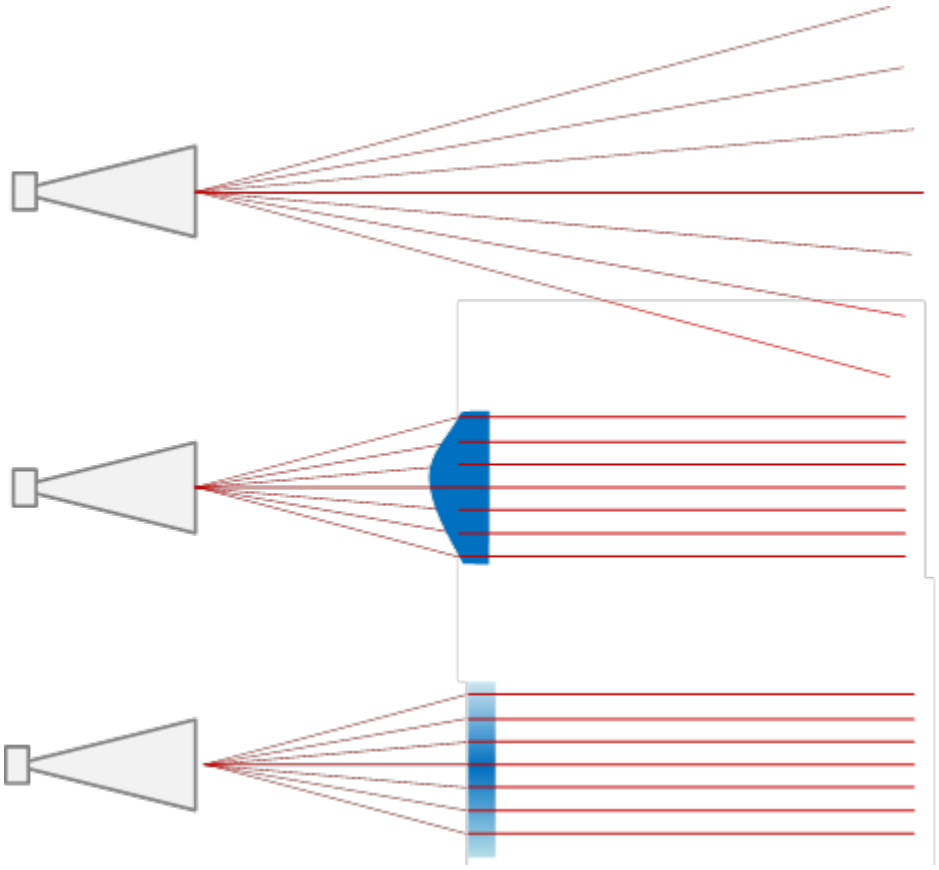

Figure 5.1 Top: Radiation from an antenna can be illustrated as radial beams originating from the antenna phase center.
Middle: A lens can align all beams, focusing the radiation, but at microwave frequencies and practical permittivity values, it must be thick
Bottom: A lens with variable refractive index can affect the radiation in the same way as a fixed permittivity lens, but the lens can in this case be much thinner

5.1 Simulations

To simulate the performance of the antenna alone, the software HFSS was again applied. The geometric model of the antenna is shown on the left side of Figure 5.2. The EM fields in the antenna and the resulting radiation diagram can then be simulated. E-field simulations at 12 GHz are shown on the right side of Figure 5.2, and the radiation diagram at 12 GHz is shown in Figure 5.3.

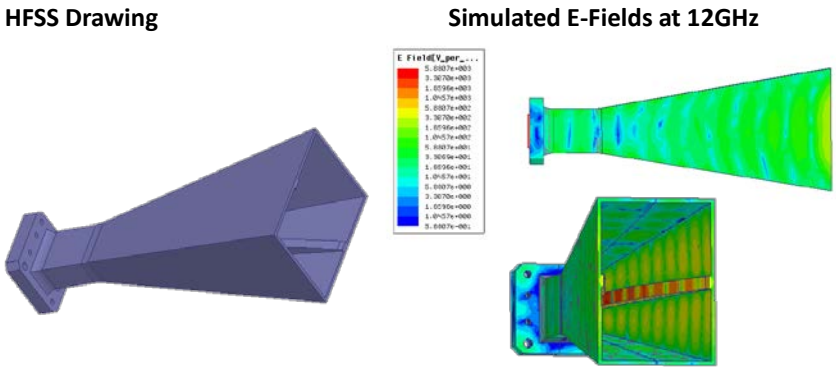

Figure 5.2 Geometric model of the horn antenna (left), and the simulated E-fields at 12 GHz (right).

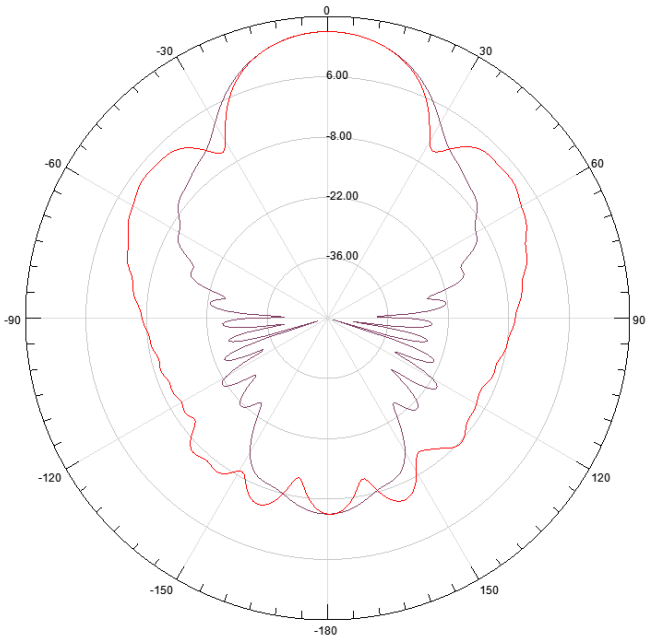

Figure 5.3 Simulated radiation pattern at 12 GHz in E-plane (blue) and H-plane (red).

For the lens we again used the 0.7 mm wire thickness to produce a lattice, but this time the cube size was a function of radial distance from the center of the object, as showed in Figure 5.4. This produces radially variable permittivity. The theory presented in [16] allows us to calculate the required ε_r versus radial distance for a given lens thickness and focal length.

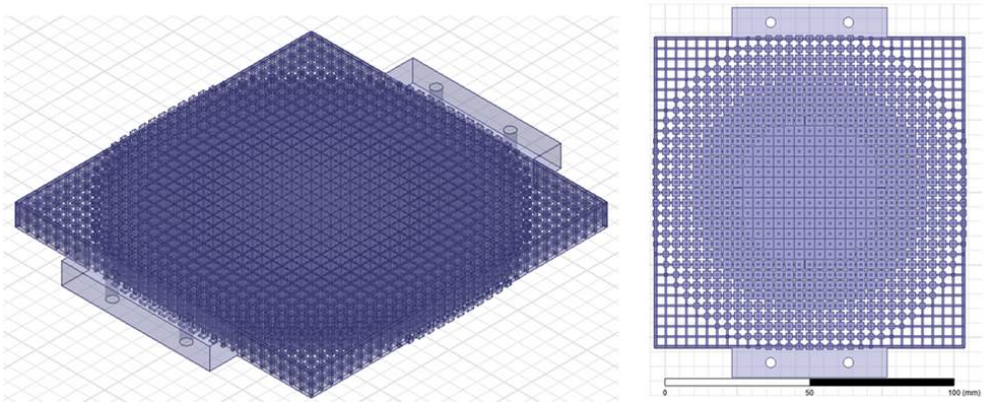

Figure 5.4 Geometric model of a three-layer lens.

Performing simulations to calculate the radiation diagram for this lens is very computationally intensive, and at the moment of writing, sufficient computer resources are not available. Due to this limitation, we do not have any simulation results, showing the effect of the lens on the radiation diagram. Thus, we had to rely on the theory behind, and on producing a number of lenses with slightly varying characteristics, which then are tested experimentally.

5.2 Measurements

The antenna radiation diagram, with and without the lens, was measured in an anechoic chamber at the University of Oslo. The measurements set-up consists of a transmitting antenna, which is fed with an RF signal. The antenna under test (AUT) was mounted, with and without lens, on a pedestal. The transmitted RF signal was swept over a preprogrammed frequency range, and the AUT was rotated horizontally through a preprogrammed range of pointing directions (± 180° in this case). For each frequency and pointing direction the received power level was stored, thus recording the radiation diagram. The measurement set-up with the lens mounted is shown on the left in Figure 5.5. The lens itself is shown on the right.

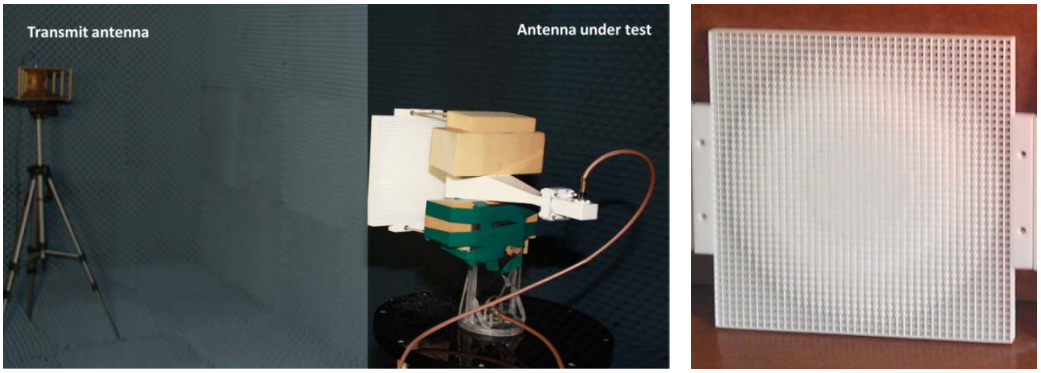

Figure 5.5 Measurement setup with antenna and lens (left), and metamaterial lens (right).

The E- and H-plane measurements were done on ten different lenses at two different distances from the antenna, and with two different antennas, resulting in a total of 84 measurements. Also, all measurements were repeated for cross-polarized transmitting signals. The full analysis of this dataset is outside the scope of this report. Here we will only report the measurement results from the antenna and lens shown in Figure 5.5.

Figure 5.6 shows measured boresight gain versus frequency for the antenna alone (red curve) and with the lens mounted at the focal distance (blue curve). Also shown in this figure is the measured gain when the lens is mounted at the antenna aperture. The lens can be seen to result in a fairly frequency independent gain of about 3dB (= double power) over the entire frequency range from 8 to 18 GHz (blue versus red curve). When the lens is mounted at the antenna aperture, all the radiation has to pass through the lens (green curve). In this case there is no gain, but more importantly, there is also very little loss. The possibility to produce a low loss lens is one of the main reasons for using the chosen metamaterial approach.

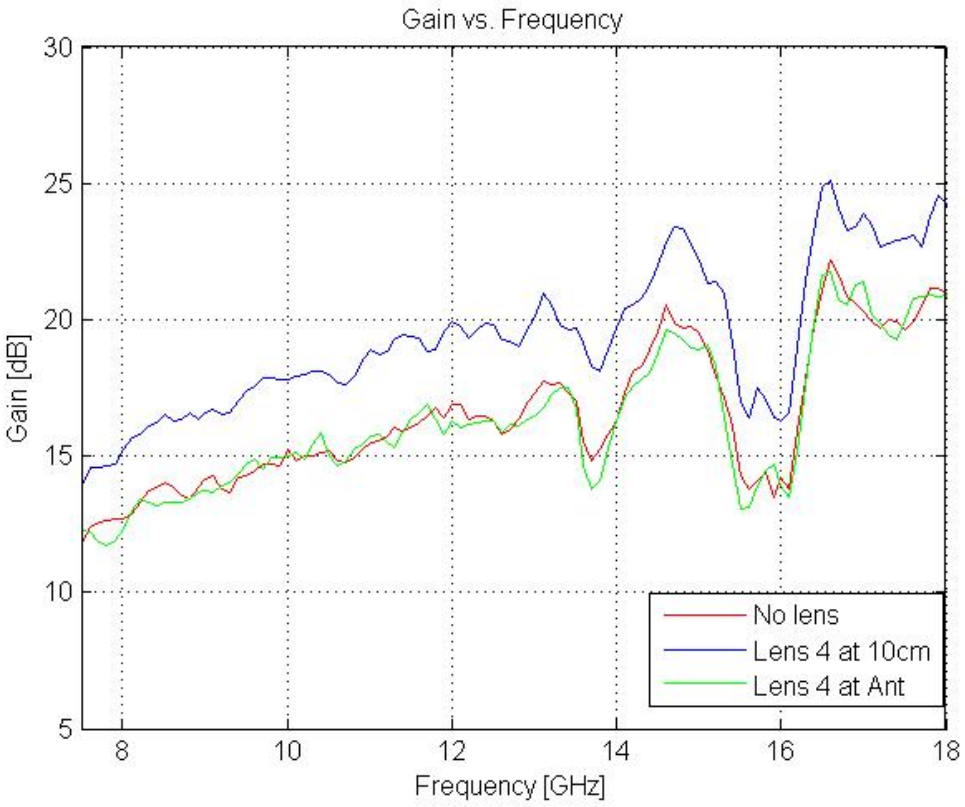

Figure 5.6 Measured boresight gain without lens (red curve) and with lens (blue curve). Also plotted is the measured gain with the lens mounted at the antenna aperture (green curve).

Another way of displaying antenna measurement results is shown in Figure 5.7. The figure shows antenna gain versus pointing angle in the H-plane (large antenna dimension) for the same three situations for three frequencies; 10, 14 and 18 GHz. Again the red curve is for the antenna alone, the blue curve for antenna with lens at focal distance, and the green curve with antenna at aperture. These plots show how the beam width of the antenna becomes narrower when the lens is used correctly. Again the green curve shows that there is little loss through the lens.

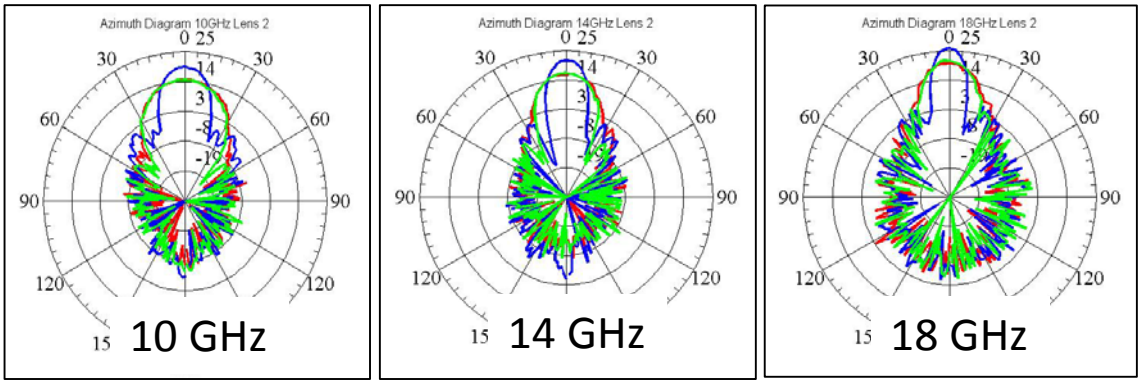

Figure 5.7 Measured E-plane radiation diagram without lens (red) and with lens (blue) at 10 (left), 14 (middle) and 18 GHz (right).

The results presented above are from an arbitrarily chosen lens out of the ten measured. There is some variation in the measurements. However, the chosen lens results are representative for the whole series, with a performance close to the average performance for this test series.

6 Experiences from the study

During this work, we came across a number of issues which are worth mentioning, and may be relevant for future work in this area.

3D printing is still considered a novel production technique, but for plastic material the process and quality of the printed parts are becoming high. However, producing the fine grid with the different size cubes at the intersections was experienced to be far from easy. The first process we tried, SLA, has been advertised to provide more than required precision and resolution, but the results were very disappointing, see Figure 6.1. We had to change to the more expensive process of SLS to be able to get acceptable quality grids, and we had to go for a 0.7 mm line thickness, which slightly affects the minimum achievable permittivity, as shown in Figure 4.6. The production was done in cooperation with the relatively newly established Addlab at NTNU Gjøvik. As they get more experienced, the product quality may increase.

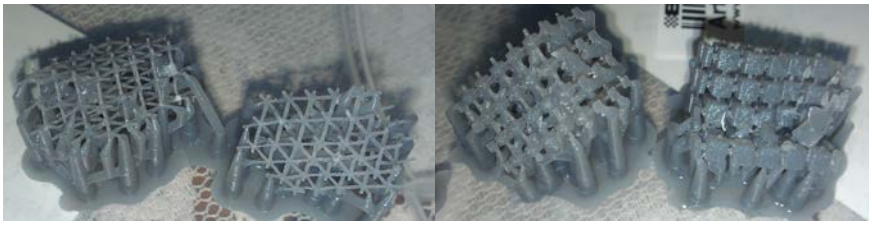

Figure 6.1 Failed attempts at producing 3D printed objects with different densities(SLA)

It was hard to obtain the correct value for ε_r for the plastic material that was used for printing. The first value we got turned out to be for another version of the material, and even for the correct version there is considerable variation between sources. This is also our experience with other polymer-based materials, like e.g. ABS. Also one cannot expect to achieve all possible variations in ε_r in reality, since there are limits on minimum and maximum achievable density. This will probably vary a lot between different 3D printing methods, as well.

This study was financed with 100.000 NOK total budget, including both work hours and investments. In reality, the number of work hours is at least the double. Additional funding has been available through the PhD work of Karina V. Hoel financed by the OPEK IV project at FFI. Also the 3D printed parts were purchased at far less than market price, due to the cooperation between OPEK IV and NTNU Gjøvik.

7 Conclusions and future work

In this work we have studied one application of metamaterials to the field of antenna design: Flat dielectric lens based on spatially varying permittivity for broad band focusing of EM radiation. The hypothesis was (supported by previous literature) that there is a systematic and predictable connection between the density and the permittivity of polymer-based materials. First we conducted a broad literature study, from which selected parts are reported here. Then we designed and produced blocks made of different density. The actual production was done at Addlab, NTNU in Gjøvik using a latest generation 3D printer.

A dielectric lens produced from a slab of material with homogenous permittivity becomes very bulky and inherently has high loss. Transformation optics allows for transforming a homogenous permittivity lens to a variable permittivity lens which can be made much thinner, and potentially much less lossy. We designed 10 different such lenses, and through simulations and measurements demonstrated that they can indeed result in increased gain and narrower antenna beams.

During the work an interesting and novel idea emerged: “Is there a potential for improving the antenna performance by introducing the same type of metamaterial *inside* the antenna?” We did not have the computing resources to simulate this, but through the good cooperation with NTNU Gjøvik we were able to produce 3D printed object literally over the weekend. Therefore we decided to produce a test lens which simply had a linearly varying density through the horn depth, with 100% density at the aperture, see Figure 7.1. This did not have a beneficial effect on the antenna performance (it actually resulted in 2-3 dB attenuation across the bandwidth). We do, however, think that there is potential in this concept, and we will continue work on this topic when new simulation capabilities are established in early 2017. This also demonstrated some issues with realizing the variable density inside larger objects, related to how to remove excess powder, which needs further study.

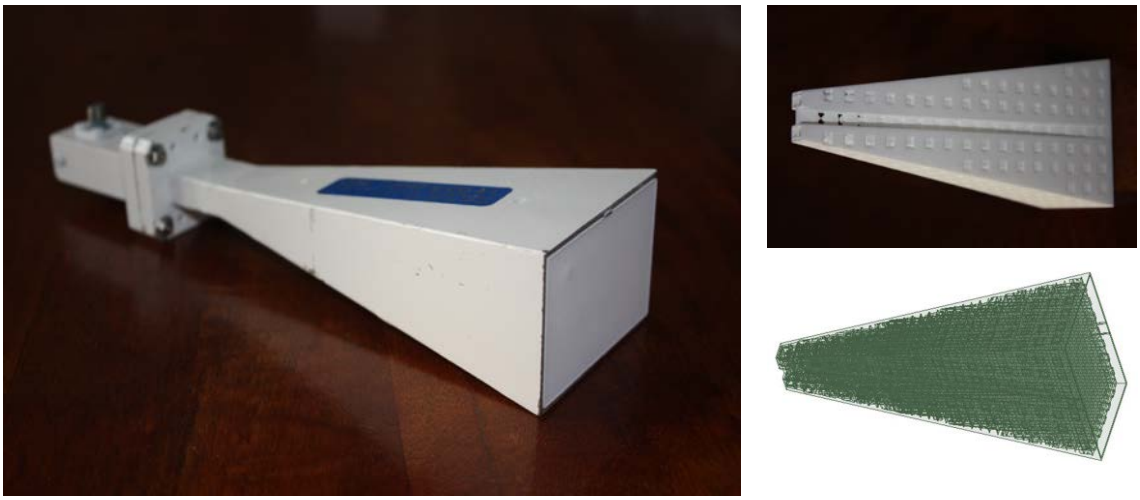

Figure 7.1 Metamaterial "lens" inside horn antenna.

References

[1] S.V Marshall, G. G.Skitek, *"Electromagnetic Concepts and Applications"*, Prentice-Hall, Third edition, 1990

[2] D. Fleisch, "A Student's Guide to Maxwell's Equations", Cambridge University Press, 2008

[3] H. Kodama, *"Automatic method for fabricating a three-dimensional plastic model with photo-hardening polymer,"* Review of Scientific Instruments, Vol. 52, No. 11, pp 1770-1773, November 1981.

[4] C.W. Hull. Apparatus for production of three-dimensional objects by stereolithography, US Patent 4575330, 1986.

[5] http://i.imgur.com/TkUOxBu

[6] P. I. Deffenbaugh, *"3D Printed Electromagnetic Transmission and Electronic Structures Fabricated on a Single Platform Using Advanced Process Integration Techniques"*, Master Thesis, Department of Electrical and and Computer Engineering, University of Texas, El Paso, 2014.

[7] Gibson, Ian, and Jorge Bártolo, Paulo. *"History of Stereolithography."* Stereolithography: Materials, Processes, and Applications. (2011): 41-43. Web. 7 October 2015

[8] http://www.stratasys.com/3d-printers/technologies/polyjet-technology

[9] http://3dvz.com/3D-granular-binding

[10] http://www.livescience.com/40310-laminated-object-manufacturing.html

[11] http://www.edn.com/design/pc-board/4427506/2/What-are-molded-interconnect-devices- (last visited 27 Jan 2017)

[12] D.V. Isakov, Q. Lei, F. Castles, C.J. Stevens, C.R.M. Grovenor, P.S. Grant: *"3D printed anisotropic dielectric composite with meta-material features"*, Materials and Design 93 423–430, (2016)

[13] C. R. Garcia1, J. Correa1, D. Espalin, J. H. Barton1,R. C. Rumpf1, R. Wicker, and V. Gonzalez:*"3D printing of anisotropic metamaterials"*, Progress In Electromagnetics Research Letters, Vol. 34, 75-82, (2012)

[14] F. Castles, D. Isakov, A. Lui, Q. Lei, C. E. J. Dancer, Y. Wang, J. M. Janurudin, S. C. Speller, C. R. M. Grovenor, P. S. Grant: *"Characterisation of 3D-printed, BaTiO3/ABS polymer composites"*, www.nature.com/scientificreports/

[15] M. Liang, W. Ng, K. Chang, K. G, M. Gehm, H. Xin: *"A 3-D Luneberg lens Antenna Fabricated by Polymer Jetting Rapid Protyping"*, IEEE Transactions on Antennas and Propagation, vol 62, No 4, April 2014

[16] S. Zhang, Y. Vardaxoglou, W Wittow, R Mittra: *"3D-printed flat lens for microwave applications*, Presented at the Antenna and Propagation Conference (IEEE LAPC2015), Loughborough, UK, (2015)

[17] F. Meng, R Liu, K Zhang, D Erni, Q Wu, L Sun, L. Li: *"Autmatic design of broadband gradient index metamaterial lens for gain enhancement of circularly polarised antennas"*, Progress in Electromagnetics Reasearch, Vol 141, 17-32, (2013)

[18] L. Varga, *"Radar signature control using metamaterials"*, Defence R & D Canada, DRDC Ottawa TM 2004-265 (2004)

[19] B. Chambers, A. Tennant: *"The phase switched screen"*, IEEE Antennas and Propagation Magazine, Vol 46, No 6 (2004)

[20] B. Chambers, K.L. Ford, A. Tennant: *"Active coating for wind turbine blades"*, Presented at the Antenna and Propagation Conference (IEEE LAPC2008), Loughborough, UK, (2008)

[21] Y. Dong, T. Itoh: *"Metamaterial-based antennas"*, Proceedings of the IEEE, Vol 100, No 7, (July 2012)

[22] N. Chamanara, C. Caloz: *"PML inspired transparent materials"*, Proceedings from IEEE AP-S 2016, 109-110 (2016)

[23] Schultz et al.: *"Radome compenzaton usingmatched negative index or refraction materials"* US patent no 6,788,273 B1, (September 2004)

[24] N Michishita, Y. Yamada: *"Metamaterial radome composed of negative refractive index lens for mobile base station antennas", Presented at IEEE ATC'14, (2014)*

[25] www.kymetacorp.com (last visited 27 Jan 2017)

[26] www.intellectualventures.com/inventions-patents (last visited 27 Jan 2017)

[27] www.echodyne.com (last visited 27 Jan 2017)

[28] http://www.avid3dprinting.com/wp-content/uploads/2015/02/DuraForm_PA.pdf
(last visited 10 Feb 2017)

[29] http://web.mit.edu/2.75/resources/random/RP_matl_2009.pdf
(last visited 10 Feb 2017)

Appendix

A Announcement on FFIs internal network «Innsiden»

Vil du gjøre en utforskende studie om metamaterialer?

Kompetanseområde Materialteknologi setter i år av inntil 100 000 kroner til en «utforskende studie» og oppfordrer forskere og ingeniører til å søke om støtte til en slik studie.

 *Tom Thorvaldsen* *Sist oppdatert: 04 mai 2016*

Det utforskende studiet må handle om et tema eller et fagområde som anses som nytt og kanskje noe umodent, men som likevel kan ha et stort potensial og gi nye muligheter for Forsvaret i fremtiden. Tema for årets studie er *metamaterialer*. Metamaterialer kan defineres som materialer som er satt sammen på en måte som ikke finnes i naturen, og som har mer spesielle egenskaper.

Søknadsfrist er fredag 27. mai 2016.

En mulig «kick-starter»

Kompetanseområde Materialteknologi ønsker i år å prøve ut en ny aktivitet for å heve kompetansen innen materialteknologi ved instituttet, og samtidig støtte nye ideer og initiativer fra forskere og ingeniører. Det er satt av inntil 100 000 kroner av kompetanseområdets midler til det som er kalt en «utforskende studie». En mer fokusert studie med konkrete mål og leveranser tror vi er mer hensiktsmessig bruk av tid og ressurser enn mer generelle kollokvier, presentasjoner eller annen informasjonsutveksling. Studien skal ikke på noe vis være konkurrerende med aktivitetene i prosjektene i linjen, men skal være et supplement til prosjektaktivitetene – en slags «kick-start» for et potensielt nytt, fremtidig prosjekt.

Generelt er noen teknologier for nye og lite definerte til at verken FFI internt eller Forsvaret er villig til å prioritere slik forskning foran andre mer modne teknologier (Det finnes selvsagt unntak!). Disse midlene er tenkt å bidra til å realisere noen av de

mulighetene som ikke nådde helt opp i konkurransen med andre prosjekter i år, men som kan bli viktige de kommende årene.

Slik søker du

Søknaden sendes til Kompetanseansvarlig Materialteknologi (KA) Tom Thorvaldsen. Søknadsfristen er fredag 27. mai 2016. Kort tid etter vil det beste forslaget annonseres, slik at arbeidet formelt kan starte opp i begynnelsen av juni.

Søknaden skal være på maksimum to A4-sider og skal inneholde:

- arbeidstittel for studien
- avgrensning av tema
- hvilke mål som ønskes oppnådd gjennom studien
- en kort bakgrunn for gjennomføringen av studien (tidligere prosjekter, relevant litteratur, muligheter for Forsvaret og lignende)
- en kort presentasjon av de som skal gjennomføre studien
- gjennomføringsplan i form av et tidsskjema (Gantt-diagram). Tidsrammen er juni til desember 2016.
- Budsjett (reisekostnader, timer, innkjøp av materialer, interne tjenester hos PtV med videre)

Følgende leveranser er forventet:

- en teknisk-faglig FFI-rapport som beskriver resultatene av studien
- presentasjon for Kompetanseområde Materialteknologi. Presentasjonen skal holdes innen utgangen av februar 2017.

Hvis det er relevant kan studien eventuelt rapporteres i form av en konferanse- eller journalartikkel. Det er ikke noe krav om at konferansebidraget eller journalartikkelen skal være innsendt (og da heller ikke publisert) innen utgangen av 2016, men manuskriptet skal være skrevet på artikkelform og være nær ved å kunne sendes inn. Eventuell deltakelse på konferanse må da tas av tildelte midler (og fremgå i budsjettet for studien), eller finansieres fra andre kilder.

KA Materialteknologi vil bistå under studien. Arbeidsprosessen og sluttresultatet vil vurderes av KA Materialteknologi, i samarbeid med avdelingssjef og forskningssjef ved avdeling Landsystemer.

B Application for the grant

3D-printet mikrobølgelinse med metamaterialegenskaper

Avgrensning av tema

Studien vil behandle linser som opererer på elektromagnetiske (EM) bølger i mikrobølgeområdet (1-40GHz), og som kan produseres vha av 3D-printing. Vi vil se på EM-egenskapene til plastmaterialet, og hvordan vi kan påvirke dem ved å variere strukturen og tettheten inne i plastlinsen. Særlig er vi interessert i å produsere romlig «programmerbar» permittivitet, ε, slik at vi kan kontroller brytning i linsen.

Arbeidet kommer til å omfatte EM-simuleringer i HFSS og produksjon vha 3D-printer av utvalgte eksempelstrukturer for måling. Vi ønsker også å lage minst en fungerende linse som vi kan bruke sammen med hornantenner som vi tidligere har produsert med 3D-printing. Målinger vil da (forhåpentligvis) kunne vise at linsen gir antennen forbedrede egenskaper.

Konkrete mål med studien

- Øke kunnskap om hvordan man kan produsere metamaterialer ved å variere struktur inne i 3D-printede plastobjekter
- Studere 3D-printede mikrobølgelinser, noe som er en av mange mulige anvendelser av metamaterialer i antenner
- Demonstrere forbedrede egenskaper for en allerede eksisterende hornantenne

Bakgrunn

Ett av de mest lovende anvendelsesområdene for metamaterialer er innen antenner. Et google-søk på '*antenna metamaterial* ' gir 364.000 treff, på google scholar får mer enn 30.000.

Antennedesign er ofte begrenset eller styrt av materialegenskaper. Materialer med nye egenskaper kan gi nye muligheter, f eks:

- Mindre antenner med samme ytelse
- Bedre ytelse uten økt størrelse
- Mer effektive antenner (mindre tap)
- Mindre kobling mellom enkeltelementer (i gruppeantenner)
- Linser på relevante frekvenser med anvendbar størrelse og akseptable tap
- Mer bredbåndede antenner

Antennedesign er også begrenset av hva som er praktisk mulig å produsere. Her har 3D-printing gitt nye muligheter. Google scholar gir ca 1.300 treff på '*antenna "3D-printed"*'. 3D-printing gir mulighet til å produsere svært komplekse strukturer, og nylige arbeider gjort av bl a søkerne viser at metallisering av plastmaterialene kan gi samme egenskaper som metall, hvis det er ønskelig.

Kombinasjonen av 3D-printing og metamaterialer er veldig interessant for antennedesign.

Søkerne har arbeidet med 3D-printede antenner det siste 1 ½ året, og publisert tre konferanseartikler på temaet (vedl 1,2,3). Dette arbeidet har ført oss mot metamaterialer siden vi nå fokuserer på en bølgeledertype som kalles «Ridge Gap Waveguid»e, og som gjør enkel bruk av et metamateriale (vedl 4,5). Denne sommeren vil det bli arbeidet videre med en arrayantenne og en spesiell type mikrobølgelinse (Rotman-linse) basert på denne type waveguide. Dette arbeidet har gitt oss erfaring i simulering, produksjon og måling på komponenter av lignende type som vi foreslår i denne studien.

Andre har tidligere gjort interessante arbeider på mikrobølgelinser, noen få også med linser produsert av 3D-printer (vedl 6,7,8), men her er det mye ugjort foreløpig.

Deltagere

Karina Vieira Hoel: Karina er OPEK-prosjektets ekspert på mikrobølgelektronikk. Hun har arbeidet innen dette området i mer enn 15 år, hvorav 10 år på FFI med utvikling av mikrobølgehardware for radarjamming. Hun jobber for tiden 50% på utvikling av neste generasjons radarjammer og 50% med PhD innen 3D-printing og mikrobølgelektronikk.

Stein Kristofferen: Stein er fagansvarlig for radar-EK i prosjekt OPEK, og faglig samarbeidspartner på Karinas PhD-arbeid. Han har jobbet på FFI med radarjamming i over 20 år.

Gjennomføringsplan

Arbeidet kan ikke starte før 1. august fordi Karina er på utenlandsopphold denne sommeren og Stein er opptatt med feltforsøk. Karina kommer tilbake medio august, men teori/litteraturstudie-arbeidet kan starte noe før.

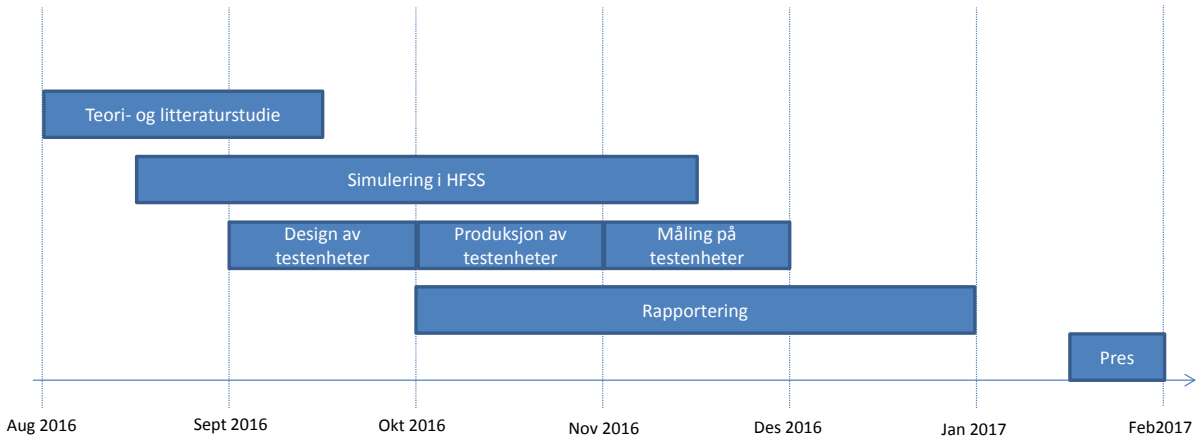

Budsjett

Her har vi ikke konkrete tall å komme med, men:

- Passende antall arbeidstimer for Karina og Stein
- Noen timer støtte fra PtV og produksjon av noen 3D-printede objekter
- Evt reiser kan taes over annet budsjett

Finansieringen kan kombineres med eksisterende finansiering for prosjekt OPEK IV.

C Maxwell's equations

Differential form

$$\nabla \times \bar{E} = -\mu \frac{\partial \overline{H}}{\partial t}$$

$$\nabla \times \bar{H} = \overline{J_c} + \epsilon' \frac{\partial \overline{E}}{\partial t}$$

$$\nabla \cdot \overline{D} = \rho$$

$$\nabla \cdot \overline{B} = 0$$

Integral form

$$\oint_l \bar{E} \cdot \bar{\partial} l = -\int_s \frac{\partial \overline{B}}{\partial t} \cdot \overline{ds} = emf$$

$$\oint_l \bar{H} \cdot \bar{\partial} l = -\int_s \left(\overline{J_c} + \frac{\partial \overline{D}}{\partial t} \right) \cdot \overline{ds} = I_{en}$$

$$\oint_S \overline{D} \cdot \overline{ds} = Q_{en} = \int_v \rho_v dv$$

$$\oint_S \overline{B} \cdot \overline{ds} = 0$$

About FFI

The Norwegian Defence Research Establishment (FFI) was founded 11th of April 1946. It is organised as an administrative agency subordinate to the Ministry of Defence.

FFI's MISSION

FFI is the prime institution responsible for defence related research in Norway. Its principal mission is to carry out research and development to meet the requirements of the Armed Forces. FFI has the role of chief adviser to the political and military leadership. In particular, the institute shall focus on aspects of the development in science and technology that can influence our security policy or defence planning.

FFI's VISION

FFI turns knowledge and ideas into an efficient defence.

FFI's CHARACTERISTICS

Creative, daring, broad-minded and responsible.

Om FFI

Forsvarets forskningsinstitutt ble etablert 11. april 1946. Instituttet er organisert som et forvaltningsorgan med særskilte fullmakter underlagt Forsvarsdepartementet.

FFIs FORMÅL

Forsvarets forskningsinstitutt er Forsvarets sentrale forskningsinstitusjon og har som formål å drive forskning og utvikling for Forsvarets behov. Videre er FFI rådgiver overfor Forsvarets strategiske ledelse. Spesielt skal instituttet følge opp trekk ved vitenskapelig og militærteknisk utvikling som kan påvirke forutsetningene for sikkerhetspolitikken eller forsvarsplanleggingen.

FFIs VISJON

FFI gjør kunnskap og ideer til et effektivt forsvar.

FFIs VERDIER

Skapende, drivende, vidsynt og ansvarlig.

FFI's organisation

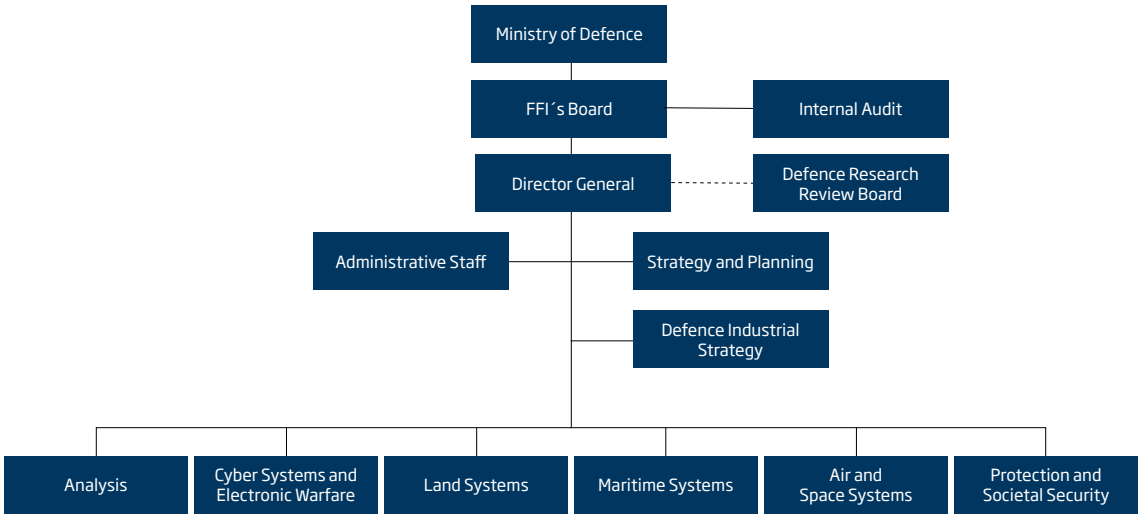

Forsvarets forskningsinstitutt
Postboks 25
2027 Kjeller

Besøksadresse:
Instituttveien 20
2007 Kjeller

Telefon: 63 80 70 00
Telefaks: 63 80 71 15
Epost: ffi@ffi.no

Norwegian Defence Research Establishment (FFI)
P.O. Box 25
NO-2027 Kjeller

Office address:
Instituttveien 20
N-2007 Kjeller

Telephone: +47 63 80 70 00
Telefax: +47 63 80 71 15
Email: ffi@ffi.no

FFI Forsvarets forskningsinstitutt
Norwegian Defence Research Establishment